JAAS

Accepted Manuscript

This is an *Accepted Manuscript*, which has been through the Royal Society of Chemistry peer review process and has been accepted for publication.

Accepted Manuscripts are published online shortly after acceptance, before technical editing, formatting and proof reading. Using this free service, authors can make their results available to the community, in citable form, before we publish the edited article. We will replace this *Accepted Manuscript* with the edited and formatted *Advance Article* as soon as it is available.

You can find more information about *Accepted Manuscripts* in the Information for Authors.

Please note that technical editing may introduce minor changes to the text and/or graphics, which may alter content. The journal's standard Terms & Conditions and the Ethical guidelines still apply. In no event shall the Royal Society of Chemistry be held responsible for any errors or omissions in this *Accepted Manuscript* or any consequences arising from the use of any information it contains.

ROYAL SOCIETY OF CHEMISTRY

www.rsc.org/jaas

Topography effect can be reduced by increasing transfer optics magnification in high precision SIMS isotope analysis.

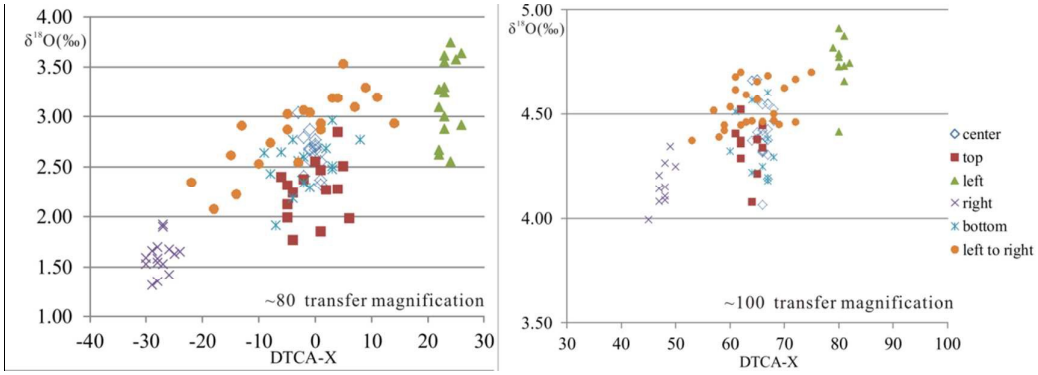

Version - 28 February 2015

Deciphering physical mechanism of topography effect for oxygen isotope measurements using Cameca IMS-1280 SIMS

Guo-Qiang Tang[1], Xian-Hua Li[1,*], Qiu-Li Li[1], Yu Liu[1], Xiao-Xiao Ling[1], and Qing-Zhu Yin[2]

[1]State Key Laboratory of Lithospheric Evolution, Institute of Geology and Geophysics, Chinese Academy of Sciences, Beijing 100029, China

[2] Department of Earth and Planetary Sciences, University of California at Davis, One Shields Avenue, Davis, CA 95616, USA

*Corresponding author
E-mail: lixh@gig.ac.cn
Phone: 86-10-82998512
Fax: 86-10-62010846

Abstract

Surface condition of sample mount is an important factor influencing the precision of SIMS isotope analysis. The phenomenon that sample topography affects analytical precision is called the topography effect. We carried out a systematic experiment of O-isotope analyses using Cameca IMS-1280 SIMS to quantitatively characterize the topography effect with the aim for a better understanding of its physical mechanism underlying such an artifact and ultimately improving the analytical precision. Our results indicate that within a mineral grain, the topography effect is obvious in X-direction (horizontal direction) of the sample stage but insignificant in Y-direction (vertical direction). In addition, within a single mineral grain, the topography effect makes analytical spots on the left rim (lower X-coordinates) yielding higher measured $\delta^{18}O$ values than those on the right rim (higher X-coordinates) in our instrument. The physical reason that topography effect compromises analytical reproducibility is attributed to lateral energy dispersion of secondary ions caused by surface topography changing the ions position in entrance slit plane. By increasing the transfer optics magnification, the topography effect could be significantly reduced. Beam centering parameters could be used to quantitatively assess topography effect and improve the data quality.

Key words: secondary ion mass spectrometer, beam centering, oxygen isotope, topography effect, analytical precision

1 Introduction

The large radius magnetic sector secondary ion mass spectrometry (SIMS) has been playing important roles in geosciences research, for its high resolution, high sensitivity and in situ analysis ability. The routine external precision of oxygen isotope ratio analysis using Cameca IMS-1280/HR SIMS is better than 0.15‰ (1SD).[1] However, it is well known that reproducibility of isotopic ratios is affected by such factors as sample geometry, sample surface topography and crystal orientation of certain minerals.[2-5] Generally, before SIMS analysis, sample grains are embedded into epoxy resin, polished and coated with gold or carbon to ensure its smooth surface to be conductive and avoid charging. Surface topography could develop during sample mount polishing process. Sample grains usually have higher surface topography than the epoxy plane after polish because of hardness difference between them. So the sample mount surface is not a perfect flat plane but a plane with many "plateaus", or surface relief.[3] For relatively "soft" minerals such as apatite (Mohs hardness = 5), the height difference between sample grains and epoxy plane is very small (~1μm), while for the "hard" minerals such as zircon (Mohs hardness = 8), it is difficult to avoid surface relief at mineral boundaries, which usually exceeds 5μm. Surface relief could cause analytical artifacts as demonstrated by previous studies.[3, 6, 7] Kita *et al* performed a detail investigation to document the influence of sample geometry and topography to the analytical precision of O-isotope measurements during SIMS analysis.[2, 3, 5] These authors called the analytical artifacts as a function of the sample

location as the "X-Y effect", and from the sample surface relief as the "topography effect". The X-Y effect can be overcome by confining sample grains within the mount center or by using a large front surface sample holder.[1] The surface relief, however, is difficult to be completely eliminated, thus, the analytical artifact caused by topography effect still persists.[2, 3, 5]. This compromises applications where the analyses on the sample rims are required, e.g., the metamorphic rims overgrown on the igneous zircon cores.

In order to better understand the mechanism of topography effect and overcome its influence on high-precision SIMS isotope analysis, we carried out a systematic experiment of O-isotope analyses using Cameca IMS-1280 SIMS to quantitatively characterize the topography effect. Our experimental results demonstrate that the topography effect is obvious in X-direction (horizontal direction) but insignificant in Y-direction (vertical direction). We show that using higher transfer optics magnification can significantly reduce the topography effect.

2 Experiments and analytical methods

Zircon mount preparation and SIMS oxygen isotope measurements are accomplished at SIMS laboratory of the Institute of Geology and Geophysics, Chinese Academy of Sciences (IGG-CAS) in Beijing. Three sessions (session 1, 2, 3) are carried out using two sample mounts (Mount A and Mount B). Mount A is used in

session 1, and Mount B in session 2 and 3. In these sessions, two oxygen isotopes (^{16}O and ^{18}O) are measured with two faraday cups using Cameca IMS-1280 SIMS. The standard deviation (SD) of multiple analyses is used as an indicator for external precision (analytical reproducibility). To evaluate the influence of surface relief to analytical reproducibility in these three sessions, a number of analyses are targeted at zircon crystal rims where surface reliefs are most significant. Analytical reproducibility in three sessions is demonstrated by analyses targeting around the center of zircon crystals, where zircon surface is fairly flat, so that the surface topography effect is negligible. Analyses in session 2 and 3 on Mount B were performed to investigate the correlation between the measured O-isotope ratio and the secondary ion beam centering parameters. Very attention is paid to the orientation of the Mount B in sample holder in session 2 and 3, which is almost exactly the same in both sessions. After session 2, Mount B is re-polished, cleaned, recoated with Au for analysis in session 3. However, the surface reliefs of the mount measured with white light profiler in both sessions are ~10μm. The details of analytical condition are list in Table 1. Note that the instrument configuration used in sessions 1 and 2 is the same, whereas, a higher transfer optics magnification is used in session 3 to test if the topography effect can be reduced.

2.1 Sample mount description

Mount A and B were prepared using the Buehler 20-8130-032 epoxy resin, and both are carefully polished using a Buehler phoenix 4000 polishing machine. Mount A contains two shards of standard zircon M257, which is a gem-quality zircon megacrystal used as a standard for U-Pb, O and Li isotope micro analytical measurements.[8, 9] The sizes of the two shards are ~1mm x 1mm and ~1mm x 2mm. The relief of this mount surface is ~5μm as measured by white light profiler. Mount B contains a single grain of standard zircon Penglai (~4mm x4 mm in size). The Penglai zircon is homogeneous in oxygen isotope composition at ~20 micron scale, and used as standard in zircon oxygen isotope SIMS analysis at our SIMS laboratory.[10]

2.2 Analytical methods

The Gaussian focused Cs^+ ions are used as primary beam to sputter zircon for O-isotope analysis. Primary beam size is ~10μm in diameter, and 2.5-3nA in intensity. The ^{16}O and ^{18}O ions are detected simultaneously by two faraday cups, and the currents are amplified by 10^{10} ohms and 10^{11} ohms resistors, respectively. Normal electron gun is used to keep the voltage of analysis area stable. The NMR controller is used to stabilize the magnetic field. The entrance slit is set at ~125μm; the field aperture is 5000x5000μm^2; the energy slit is 30eV, and the exit slit is ~500μm. In sessions 1 and 2, the magnification of transfer system is configured as ~80, while in session 3 this value is ~100. Because of the higher transfer optics magnification used

in session 3, the transmission efficiency of secondary ions is greatly improved. The signal intensity of ^{16}O is ~1.6×10^{9} cps (counts per second) in sessions 1 and 2 with ~3nA primary beam intensity, and is ~2.1×10^{9} cps with ~2.5nA primary beam intensity in session 3. Each spot analysis consists of pre-sputtering, beam centering in apertures, and signal collecting process. A single spot analysis spends 3 min, including 2 min for pre-sputtering and centering secondary beam and 1 min to collect 16 cycles of ^{16}O and ^{18}O signals. The $^{18}O/^{16}O$ ratios are normalized to V-SMOW ($^{18}O/^{16}O$ = 0.0020052) and expressed on the $\delta^{18}O$-scale.[11] The details of the analytical condition are list in Table 1.

2.3 Analytical results

2.3.1 Session 1

As sample surface relief can deteriorate analytical results,[3] we carried out experiments in session 1 to quantitatively examine the extent of the influence caused by surface relief. Oxygen isotope measurements are carried out on two shards of M257 zircon in Mount A, and spots positions are marked in Figure 1. At the beginning of analysis for each shard, 6 or 7 spots on the center part are measured, and then 24 and 21 spots on the zircon rims are analyzed for shard-1 and shard-2, respectively. All spots are analyzed in a single session. Analytical results and the beam centering parameters are listed in ESI Table 1 †.

Analytical uncertainty of the center spots for two shards is 0.12‰ (1SD), indicating the reproducibility of O-isotope measurement of this session. On the other hand, analytical uncertainty of rim spots for shard-1 and shard-2 are 0.69‰ and 0.55‰ (1SD), respectively, reflecting a clear topography effect that deteriorates analytical reproducibility. Figure 2 shows the coordinates of analysis spots and their measured $\delta^{18}O$ values. It can be seen that, for each shard in X-direction, the lower coordinates spots always have higher measured $\delta^{18}O$ values, consistent with the results of Kita *et al*.[3] However, such phenomenon is not observed in Y-direction. We plot the measured $\delta^{18}O$ values against secondary beam centering parameter DTCA-X (Figure 3). For analytical spots on the rim there is a clear liner trend between the measured $\delta^{18}O$ and DTCA-X values, with the coefficients (R^2) of 0.84 and 0.88 for shard-1 and shard-2, respectively. Contrarily, no clear trend is found between the measured $\delta^{18}O$ values and DTCA-X values for the center spot analyses. In order to further examine the validity of this correlation between the measured $\delta^{18}O$ values and DTCA-X values, and whether the topography effect would happen in Y-direction, we conducted a detailed, duplicate experiment in session 2.

2.3.2 Session 2

Mount B is prepared with a big, square-shaped Penglai zircon standard grain (~4mm x 4mm) embedded in the center. A total surface relief is ~10μm (Figure 4 (a)). A total of 96 spots are analyzed in session 2. Fifteen analyses were conducted on each

rim of the square grain, namely, left, right, top and bottom, and 15 around the center dispersed randomly in order to monitor the stability of the instrument. An additional, 21 spots were analyzed traversing from the right to the left, with an interval of 150μm between the two neighboring spots. All the analytical results are list in ESI Table 2 †. Spots coordinates and measured $\delta^{18}O$ values are shown in Figure 5. The analytical results of left rim, right rim, top rim, bottom rim, and the center are 3.18±0.40‰, 1.6±0.17‰, 2.26±0.29‰, 2.52±0.26‰ and 2.65±0.19‰ (1SD), respectively. The average value of the 21 spots for the right to left traverse is 2.86±0.37‰ (1SD). The 1σ standard deviation (1SD) of 15 center spots is 0.19‰ which reflects the analytical reproducibility of this session. In contrast, 1SD of other groups (except for the right rim) exceeds 0.25‰, reflecting the analytical artifact caused largely by the topography effect. 1SD of all 96 spots is 0.57‰, similar to the results in session 1. It is noticed that the average value of left rim spots is 3.18‰, which is significantly higher than average value of right rim spots 1.6‰. Thus, the topography effect is significant in X-direction within a single grain, similar to the results obtained in session 1. In Y-direction, the average $\delta^{18}O$ value of the upper rim spots (2.26±0.29‰) is 0.26‰ lower than that of the bottom rim spots (2.52±0.26‰). Considering the relatively large standard deviation, this difference is insignificant. In Figure 6 the measured $\delta^{18}O$ values of the six groups are plotted against their beam centering parameter DTCA-X values. There is a linear correlation between the measured $\delta^{18}O$ and DTCA-X values, similar to that observed in session 1 (Figure 3). For the 21

traverse spots across the whole grain, the measured $\delta^{18}O$ values are also linearly correlated with DTCA-X values.

2.3.3 Session 3

After SIMS analysis in session 2, Mount B is re-polished, cleaned, recoated with Au and used for analysis again in session 3. The orientation of the Mount B in sample holder in session 3 is nearly the same as in session 2, namely, the left rim, right rim, top rim and bottom rim in session 2 is the same as in session 3. While the analytical condition used in session 3 is slightly different from session 2. The transfer optics magnification used in session 3 is ~100, in contrast to ~80 in sessions 1 and 2 (Table 1). This change attempts to suppress the topography effect, since higher transfer magnification could decrease the beam size in entrance slit plane and improve transmission of secondary ions.[12-14] A total of 85 spots are analyzed in this session. Ten analyses are targeted on each rim of the square grain, and 24 analyses were made for a left to right traverse with a 140μm spatial interval between spots. Twenty-one spots were randomly dispersed on the center of the mount to monitor the stability of the instrument. The results are list in ESI Table 3†. Figure 7 shows the coordinates and measured $\delta^{18}O$ value of each analytical spots. The analytical results on left rim, right rim, top rim, bottom rim, and center are 4.74±0.14‰, 4.16±0.10‰, 4.34±0.12‰, 4.35±0.16‰ and 4.41±0.15‰ (1SD) respectively. The average value of the 24 traverse spots is 4.54±0.11‰ (1SD). The 1SD of center spots is 0.15‰, which reflects

the analytical stability of the session, broadly consistent with the 1SD of other groups (0.10-0.16‰). Analytical precision for all 85 measurements is 0.20‰ (1SD). It is noted that the average value of 4.74‰ for left rim analyses is still higher than the average value of 4.16‰ for right rim analyses, outside the standard deviation. Therefore, the topography effect is still apparent in X-direction in session 3, but it is not as pronounced as shown in sessions 1 and 2, demonstrating the effectiveness of transfer optics parameter in reducing the topography effect. In Y-direction, the average value of the top rim spots is the same within error to that of the bottom rim spots, indicating that the topography effect in Y-direction is insignificant. Figure 8 shows the relationship between the measured $\delta^{18}O$ values of all six groups against their beam centering parameter DTCA-X values. The 85 spots data set as a whole yield a linear trend between the measured $\delta^{18}O$ and DTCA-X values, similar to those observed in sessions 1 and 2. For the 24 traverse analytical spots from left side to right side of the grain, the measured $\delta^{18}O$ values seem unrelated with DTCA-X values, with a 1SD dispersion of 0.11‰.

3 Discussion

3.1 Analytical artifact due to surface topography

In sessions 1 and 2, the central analytical spots were located in a small area with surface relief less than 1μm. The standard deviations of these analytical spots in

sessions 1 and 2 are 0.12‰ and 0.19‰, respectively, indicating good external reproducibility in both sessions. However, the standard deviation of all other analytical spots away from the center on the same shards exceeds 0.5‰, indicating that a surface relief over 5μm will cause significant analytical artifact for rim spots. In addition, a relative large standard deviation of 0.37‰ is obtained for 21 traverse analytical spots in session 2, indicating that analytical reproducibility deteriorates due largely to rim spots away from the center in the traverse analyses. Our experimental results support the conclusion that the surface topography could cause analytical artifacts, especially on the grain edges where sample relief is obvious.[3, 7]

3.2 Topography effect in X- and Y-directions

Kita *et al* demonstrated that the sample topography yielded higher apparent $\delta^{18}O$ values for the spots at lower coordinates in both X- and Y-directions in a single zircon grain.[3] Our experimental results are consistent with Kita's observations in X-direction. In session 2, the average of left rim spots is 1.58‰ higher than average of right rims spots. The difference is reduced to 0.58‰ in session 3, although it is still significant considering smaller standard deviation of all 85 data (0.2‰) in this session.

The topography effect is not significant in Y-direction in our measurements. In session 2, the average value of the top rim spots is only 0.26‰ lower than that of the bottom rim spots. Considering the standard deviations of top and bottom rim spots are

0.29‰ and 0.26‰, respectively, the measured values of top and bottom rim spots are indistinguishable within analytical uncertainty. In session 3 the results of top rim (4.34±0.12‰) and bottom rim spots (4.35±0.16‰) are nearly identical.

To secure the compare of topography effect between session 2 and 3, we took photos of the Penglai zircon grain using a microscope after measurements to check the mount orientation in sample holder in two sessions. The photos of the grain and spots coordinates in instrument in session 2 and 3 are shown in ESI Figure 1 †. By combining the photos and the spots coordinates in SIMS instrument, we find the mount orientation in sample holder is nearly same in both sessions.

We thus conclude that the topography effect in our instrument is obvious in X-direction but insignificant in Y-direction within a single grain. Moreover, our analytical results demonstrate that the topography effect results in apparent higher $\delta^{18}O$ values for the left rim spots (lower coordinates) than those of the right rim spots (higher coordinates) in our instrument. We do not expect the same phenomenon on other same type instruments because it may be dependent on stray magnetic field in surroundings, which could be different from place to place.[6, 14]

3.3 Mechanism of topography effect

Zircon grains in this study show slightly convex surface (Figures 1, 4), which is formed during preparation of the sample mounts. The convex surface topography can

cause secondary ions formed at grain rims with lateral energy or velocities when leaving sample, because sample itself is acting as electrode of lens forming a strong electrostatic field to extract ions.[14] Lateral energy variation can influence the ion position in entrance slit plane.[6, 12] DTCA-X denotes electrostatic voltage driving octopole to correct for the lateral energy variations of secondary ions. DTCA-X scan is performed before every spot analysis to center secondary ion beam in entrance slit in X direction. This function is useful to achieve good analytical reproducibility from spot to spot, because it could stabilize position of secondary beam in entrance slit plane.[6] Secondary ions formed at grain center have very little lateral energy (velocity) dispersion because of relatively flat surface. DTCA-X scan is performed in this case to serve as a reference value. In contrast to ions formed at grain center, ions formed at left rims and right rims acquire higher lateral velocities with opposite directions, leading to their very different DTCA-X values from the reference (Figures 3, 6 and 8). Therefore, the measured $\delta^{18}O$ value was affected accordingly with the lateral energy dispersion caused by surface topography (Figures 3, 6 and 8). It is the lateral energy dispersion due to surface topography that destabilizes the beam position in entrance slit plane and deteriorate analytical reproducibility.

To exclude the possibility that re-polishing before session 3 removes the surface relief and improves the analytical reproducibility, we measure Mount B with white light profiler again after session 3, and the result is shown is Figure 4 (b). The surface relief in session 3 is nearly the same as that in session 2 (Figure 4). So the improved

analytical reproducibility in session 3 than in session 2 is attributed to higher transfer magnification used in session 3. Compared to the transfer optics magnification of 80 used in sessions 1 and 2, a higher value of 100 is used in session 3. The role of higher transfer optics magnification is to make the secondary ion beam focused on entrance slit plane.[12-14] In sessions 1 and 2, the linear relationship between measured $\delta^{18}O$ and DTCA-X values is very significant (Figures 3, 6), whereas the range of DTCA-X values is much smaller in session 3 (Figure 6). Although a visible linear relationship was not completely removed (Figure 8), analytical reproducibility is greatly improved in session 3. This is further demonstrated by the small standard deviation of 0.11‰ for traverse spots analysis in session 3, in stark contrast to that of 0.37‰ in session 2.

3.4 Beam centering parameters in Cameca IMS-1280 SIMS

On Cameca IMS-1280 SIMS, beam centering parameters - DTFA-X, DTFA-Y, DTCA-X, and DTCA-Y form double deflection transfer centering to correct the trajectory of secondary ions:. DTFA-X and DTFA-Y denote electrostatic voltages driving deflector plate to center ions in field aperture. DTCA-X, DTCA-Y denote electrostatic voltages driving octopole to center ions in contrast aperture. Because entrance slit is close to contrast aperture, and, in most cases, it is much narrower than contrast aperture in X direction, DTCA-X actually center ions in entrance slit. DTCA-Y is not as effective as DTCA-X in microprobe mode. Factors such as mount

surface topography or inclination, parasitic magnetic field change of transfer system, can make ions distribution drift in entrance slit and field aperture. Beam centering should be carried out before every spot analysis to overcome these factors.[6] Some workers have noticed the importance of beam centering.[1, 6, 7] Whitehouse *et al* summarized many possible factors that could influence oxygen isotope analysis precision and suggested that spots position and beam centering parameters should be used to assess data reliability.[7] Peres *et al* introduced a new style sample holder to improve surface area of analysis.[1] In their study beam centering values variations were used to assess performance of the holder.[1] Our experiments demonstrate that beam centering parameters can be used to assess the reliability of data. If beam centering parameters are highly variable, or correlated with the measured $\delta^{18}O$ values, the corresponding analyses should be scrutinized.

4 Conclusions

The topography effect is one of the major problems causing analytical artifacts in O-isotope measurements by using Cameca IMS-1280 SIMS. Thus, understanding the mechanism of topography effect is crucial to high precision isotope analysis. Our experimental results demonstrate that topography effect in X-direction is much more prominent than that in Y-direction within a single grain; the left rim spots (lower coordinates) show higher measured $\delta^{18}O$ values than the right rim spots (higher

coordinates) in our instrument. The topography effect is attributed to the lateral energy caused by surface topography that destabilizes the beam position in entrance slit plane and deteriorate analytical reproducibility. Increasing transfer optics magnification could largely reduce topography effect and improve analytical reproducibility. Beam centering parameters could be used to assess the reliability of data. If beam centering parameters are highly variable, or correlated with the measured $\delta^{18}O$ value, the corresponding analyses might be problematic, and the sample mount needs careful examination.

Acknowledgment

We wish to thank H.X. Ma for her assistance with mounting and polishing work in our laboratory. The work would not have been possible without her dedicated support. We also would like to thank two anonymous reviewers for their valuable suggestion and comments which have greatly improved the manuscript. This work was supported by NSFC (Grant 41173010) and State Key Laboratory of Geological Processes and Mineral Resources (GPMR201201).

Reference

1. P. Peres, N. T. Kita, J. W. Valley, F. Fernandes and M. Schuhmacher, *Surface and Interface Analysis*, 2013, **45**, 553-556. DOI: 10.1002/sia.5061.
2. N. T. Kita, J. M. Huberty, R. Kozdon, B. L. Beard and J. W. Valley, *Surface and Interface Analysis*, 2011, **43**, 427-431. DOI: 10.1002/sia.3424.
3. N. T. Kita, T. Ushikubo, B. Fu and J. W. Valley, *Chemical Geology*, 2009, **264**, 43-57. DOI: 10.1016/j.chemgeo.2009.02.012.
4. J. M. Huberty, N. T. Kita, R. Kozdon, P. R. Heck, J. H. Fournelle, M. J. Spicuzza, H. Xu and J. W. Valley, *Chemical Geology*, 2010, **276**, 269-283. DOI: 10.1016/j.chemgeo.2010.06.012.
5. M. Fayek, *Secondary Ion Mass Spectrometry in the Earth Sciences: Gleaning the Big Picture from a Small Spot*, Mineralogical Association of Canada. 2009.
6. M. Schuhmacher, F. Fernandes and E. de Chambost, *Applied Surface Science*, 2004, **231-232**, 878-882. DOI: 10.1016/j.apsusc.2004.03.157.
7. M. J. Whitehouse and A. A. Nemchin, *Chemical Geology*, 2009, **261**, 32-42. DOI: 10.1016/j.chemgeo.2008.09.009.
8. L. Nasdala, W. Hofmeister, N. Norberg, J. M. Martinson, F. Corfu, W. Dörr, S. L. Kamo, A. K. Kennedy, A. Kronz, P. W. Reiners, D. Frei, J. Kosler, Y. Wan, J. Götze, T. Häger, A. Kröner and J. W. Valley, *Geostandards and Geoanalytical Research*, 2008, **32**, 247-265. DOI: 10.1111/j.1751-908X.2008.00914.x.
9. X.-H. Li, Q.-L. Li, Y. Liu and G.-Q. Tang, *Journal of Analytical Atomic Spectrometry*, 2011, **26**, 352-358. DOI: 10.1039/c0ja00073f.
10. X.-H. Li, W.-G. Long, Q.-L. Li, Y. Liu, Y.-F. Zheng, Y.-H. Yang, K. R. Chamberlain, D.-F. Wan, C.-H. Guo, X.-C. Wang and H. Tao, *Geostandards and Geoanalytical Research*, 2010, **34**, 117-134. DOI: 10.1111/j.1751-908X.2010.00036.x.
11. P. Baertschi, *Earth and Planetary Science Letters*, 1976, **31**, 341-344. DOI: 10.1016/0012-821x(76)90115-1.
12. G. Slodzian, in *Advances in Electronics and Electron Physics*, ed. A Septier, Academic Press, New York. 1980, vol. supplement 13B.
13. A. Benninghoven, F. G. Rüdenauer and H. W. Werner, *Secondary ion mass spectrometry : Basic concepts, instrumental aspects, applications and trends*, Wiley, New York. 1987.
14. G. Slodzian, *Applied Surface Science*, 2004, **231-232**, 3-12. DOI: http://dx.doi.org/10.1016/j.apsusc.2004.03.015.

Figure Caption

Figure 1 Surface topography of M257 zircon shards in Mount A measured by white light profiler. The right is shard 1, and the left is shard 2. The analytical spot positions are marked in the figure. Through the X, Y, Z, Ranges measured by white light profiler, we can evaluate the size of the two shards and the relief condition of the mount surface.

Figure 2 Analytical spots in session 1. Measured $\delta^{18}O$ value at each spot is shown in color density with the scale bar to the right. Coordinates are from IMS-1280 SIMS and the unit is in micrometer. For each shard in X direction, the lower coordinates spots are shown to have higher measured $\delta^{18}O$ values.

Figure 3 Plot of measured $\delta^{18}O$ values against beam centering parameter DTCA-X in session 1. For rim spots, measured $\delta^{18}O$ values are highly correlated with DTCA-X.

Figure 4 Surface topography of square-shaped Penglai zircon grain in Mount B measured by white light profiler. Figure (a) and (b) demonstrate the reliefs are 12.85μm and 13.14μm during session 2 and 3, respectively. The surface relief is nearly the same in both sessions.

Figure 5 Analytical spots in session 2. Measured $\delta^{18}O$ value at each spot is shown in color density with the scale bar to the right. Coordinates are from IMS-1280 SIMS and the unit is in micrometer. Left rim spots have higher measured $\delta^{18}O$ values than right rim spots, whereas the differences of measured $\delta^{18}O$ values

between the top rim spots and bottom rim spots are not obvious.

Figure 6 Plot of measured $\delta^{18}O$ values against beam centering parameter DTCA-X in session 2. There is a clear trend between measured $\delta^{18}O$ values and DTCA-X when all 96 spots are considered together. For the 21 traverse spots (solid orange circles), the trend is most pronounced.

Figure 7 Analytical spots in session 3. Measured $\delta^{18}O$ value at each spot is shown in color density with the scale bar to the right. Coordinates are from IMS-1280 SIMS and the unit is in micrometer. Left rim spots have higher measured $\delta^{18}O$ values than right rim spots. Measured $\delta^{18}O$ values of top rim spots and bottom rim spots are indistinguishable.

Figure 8 Plot of measured $\delta^{18}O$ values against beam centering parameter DTCA-X in session 3. A general linear trend between measured $\delta^{18}O$ values and DTCA-X is still visible. However, compared with results in session 2, the DTCA-X range is smaller and analytical reproducibility is much better. Unlike that in session 2, the 24 traverse spots (solid orange circles), the linear trend is less obvious.

Table 1 Analytical condition

	Sessions 1 and 2	Session 3
Primary beam diameter	~10μm	~10μm
Primary beam intensity	~3nA	~2.5nA
Entrance slits	125μm	125μm
Contrast aperture	400μm	400μm
Max area	~100μm	~80μm

Transfer optics magnification (8000/Max area)	~80	~100
Field aperture	5000μm	5000μm
Energy slit	30eV	30eV
Exit slit	500μm	500μm
Mass resolving power	2400 (FWHM)	2400 (FWHM)
^{16}O ions intensity	~1.6×10^{9} counts/s	~2.1×10^{9} counts/s
Sensitivity	~0.53×10^{9}counts/s/nA	~0.84×10^{9}counts/s/nA